Diffractive η_c and η_b productions by neutrinos via neutral currents

A. Hayashigaki*
Department of Physics, University of Tokyo, Tokyo 113-0033, Japan

K. Suzuki†
Division of Liberal Arts, Numazu College of Technology, Shizuoka 410-8501, Japan

K. Tanaka‡
Department of Physics, Juntendo University, Inba-gun, Chiba 270-1695, Japan
(Received 4 December 2002; published 16 May 2003)

We report on a first theoretical study for neutrino-induced diffractive production of heavy pseudoscalar mesons η_c and η_b off a nucleon. Based on the factorization formalism for exclusive processes, we evaluate the forward diffractive production cross section in perturbative QCD in terms of the light-cone $Q\bar{Q}$ wave functions (WFs) of $\eta_{c,b}$ mesons and the gluon distribution of the nucleon. The light-cone WFs of the η_c (η_b) meson are constructed to satisfy the spin symmetry relations with those of the J/ψ (Υ) meson. The diffractive η_c production is governed by the axial-vector coupling of the longitudinally polarized Z boson to a $Q\bar{Q}$ pair, and the resulting η_c production rate is larger than that for the J/ψ by one order of magnitude. We also discuss the production of bottomonium η_b, which shows up for a higher beam energy.

DOI: 10.1103/PhysRevD.67.093002 PACS number(s): 12.15.Lk, 12.38.Bx, 12.39.St, 13.15.+g

Exclusive diffractive leptoproduction of neutral vector mesons provides unique insight into the interplay between nonperturbative and perturbative effects in QCD [1]. The diffractive processes are mediated by the exchange of a Pomeron with the vacuum quantum numbers, whose QCD description is directly related to the gluon distributions inside the nucleons for small Bjorken x [2–6]. The processes also allow us to probe the light-cone wave functions (WFs) of the vector mesons. Relating to the latter point, however, the applicability is apparently limited to probing the neutral vector mesons.

In this paper, we propose the exclusive diffractive production of mesons in terms of the neutrino beam. The weak currents allow us to observe both neutral (M^0) and charged mesons ($M^{\pm}$) as $\nu_\mu + N \rightarrow \nu_\mu/\mu^{\mp} + N + M^0/M^{\pm}$ by Z/W boson exchange [7,8], and these mesons can be not only vector but also other types of mesons, including pseudoscalar mesons. Thus, such processes may reveal the structure of various kinds of mesons, the coupling of the QCD Pomeron to a quark-antiquark pair with various spin-flavor quantum numbers, and information on the Cabibbo-Kobayashi-Maskawa (CKM) matrix elements. There already exist some experimental data for π, ρ, $D_s^{\pm}$, D_s^* [10,9], D_s^{*+} [11], and J/ψ production [9], but there are only a few theoretical calculations, e.g., for the J/ψ production in a vector meson dominance model [12] and for D_s^- production with the generalized parton density [13]. Our work gives a first QCD calculation for diffractive meson productions via the weak neutral current. Here, our interest will be directed to production of heavy pseudoscalar mesons, especially η_c and η_b as in Fig. 1. So far η_c has been observed via the decays of J/ψ or B mesons produced by $p\bar{p}$ and e^+e^- reactions, while η_b has not been observed. The diffractive production via the weak neutral current will give direct access to η_c as well as a new experimental method to identify η_b by, e.g., measuring the two-photon decay.

We treat the η_c and η_b productions by generalizing the approach in the leading logarithmic order of perturbative QCD, which has been developed successfully for vector meson electroproduction [2–6]. We consider the near-forward diffractive production $Z^*(q) + N(P) \rightarrow \eta_Q(q+\Delta) + N'(P-\Delta)$, where $Q=c,b$, and $q, q+\Delta, P$, and $P-\Delta$ denote the momenta of the virtual Z boson, η_Q meson, and initial and final nucleons, respectively. The total center-of-mass energy $W=\sqrt{(P+q)^2}$ is much larger than any other mass scales involved, i.e., $W^2 \gg K^2$ with $K^2 = \mathcal{Q}^2, -t, m_Q^2, \Lambda_{\rm QCD}^2$, etc., where $\mathcal{Q}^2 = -q^2$, $t=\Delta^2$, and m_Q is the heavy-quark mass. We also suppose $-t \ll m_Q^2$ and $\Lambda_{\rm QCD}^2 \ll m_Q^2$. The heavy-quark mass m_Q ensures that perturbative QCD can be applied even for $\mathcal{Q}^2=0$ to calculate the creation of the $Q\bar{Q}$ pair as well as its time development before the nonperturbative effects to form a quarkonium state η_Q set in. The crucial point is that at high W the scattering of the $Q\bar{Q}$ pair on the nucleon oc-

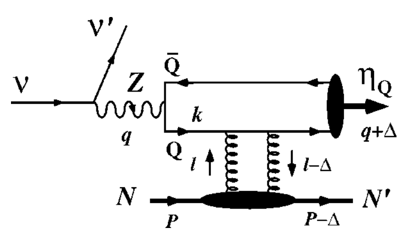

FIG. 1. A typical diagram for the exclusive diffractive $\eta_Q(Q=c,b)$ production induced by the neutrino (ν) through the Z boson exchange. There are other diagrams obtained by interchanging the vertices on the heavy-quark lines.

*Present address: Institut für Theoretische Physik der Universität, 93040 Regensburg, Germany. Electronic address: arata@nt.phys.s.u-tokyo.ac.jp
†Electronic address: ksuzuki@la.numazu-ct.ac.jp
‡Electronic address: tanakak@sakura.juntendo.ac.jp

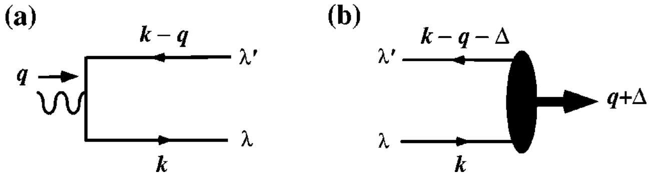

FIG. 2. Diagrams representing the light-cone WFs: (a) for the virtual Z boson; (b) for the η_Q meson.

curs over a much shorter time scale than the $Z^* \to Q\bar{Q}$ fluctuation or the $Q\bar{Q} \to \eta_Q$ formation times (see Fig. 1). As a result, the production amplitudes obey factorization in terms of the Z and η_Q light-cone WFs. The $Q\bar{Q}$-N elastic scattering amplitude, sandwiched between the Z and η_Q WFs, is further factorized into the $Q\bar{Q}$-gluon hard scattering amplitude and the nucleon matrix element corresponding to the (unintegrated) gluon density distribution. This latter step in the factorization to get the gluon distribution can be carried out in the same manner as in previous work [2–6]. The participation of the "new players" Z and η_Q in the former step requires an extension of previous work by introducing the corresponding light-cone WFs.

First of all, we discuss the extension due to the participation of the Z boson. The $ZQ\bar{Q}$ weak vertex of Fig. 1 is given by $(g_W/2\cos\theta_W)\gamma_\mu(c_V - c_A\gamma_5)$, where $(g_W/2\cos\theta_W)^2 = \sqrt{2}G_F M_Z^2$ with G_F the Fermi constant and M_Z the Z mass. $c_V = 1/2 - (4/3)\sin^2\theta_W, c_A = 1/2$ for the c quark, and similarly for the b quark. As usual, we introduce the two lightlike vectors q' and p' by the relations $q = q' - (\mathcal{Q}^2/s)p'$, $P = p' + (M_N^2/s)q'$, $q'^2 = p'^2 = 0$, $s = 2q' \cdot p'$ with M_N the nucleon mass and $s \cong W^2 + \mathcal{Q}^2 - M_N^2$, and the Sudakov decomposition of all momenta, e.g., $k = \alpha q' + \beta p' + k_\perp$.

We also introduce the polarization vectors $\varepsilon^{(\xi)}$ ($\xi = 0, \pm 1$) of the virtual Z boson to satisfy $\Sigma_\xi (-1)^{\xi+1} \varepsilon_\mu^{(\xi)*} \varepsilon_\nu^{(\xi)} = -g_{\mu\nu} + q_\mu q_\nu / M_Z^2$, which is the numerator of the propagator for the massive vector boson. Because the $q_\mu q_\nu / M_Z^2$ term vanishes when contracted with the neutral current, we conveniently choose

$$\varepsilon^{(0)} = \frac{1}{\mathcal{Q}} q' + \frac{\mathcal{Q}}{s} p', \quad \varepsilon^{(\pm 1)} = \varepsilon_\perp^{(\pm 1)} = \frac{1}{\sqrt{2}}(0,1,\pm i,0), \quad (1)$$

for the longitudinal ($\xi = 0$) and transverse ($\xi = \pm 1$) polarizations, respectively. Equation (1) coincides with the polarization vectors for the virtual photon in Refs. [2–5]. For the J/ψ electroproduction, the wavy line of Fig. 1 and Fig. 2(a) denotes a virtual photon. The corresponding photon light-cone WFs are derived as [3,4,14]

$$\Psi_{\lambda\lambda'}^{\gamma(\xi)}(\alpha, \boldsymbol{k}_\perp) = -e_Q \frac{\sqrt{\alpha(1-\alpha)}\,\bar{u}_\lambda(k) \not\varepsilon^{(\xi)} v_{\lambda'}(q-k)}{\alpha(1-\alpha)\mathcal{Q}^2 + \boldsymbol{k}_\perp^2 + m_Q^2} \quad (2)$$

with Eq. (1) for $\xi = 0, \pm 1$. Here e_Q is the electric charge of the quark, and $u_\lambda(k)[v_{\lambda'}(q-k)]$ denotes the on-shell spinor for the (anti)quark with helicity λ (λ'). These WFs describe the probability amplitudes to find the photon in a state with the $Q\bar{Q}$ pair, where the quark carries the longitudinal momentum fraction α and the transverse momentum $\boldsymbol{k}_\perp$ as $k = \alpha q' + \beta p' + k_\perp$, $k_\perp^2 = -\boldsymbol{k}_\perp^2$. Obviously, the light-cone WFs for the virtual Z boson can be obtained from Eq. (2) by the replacement $e_Q \gamma_\mu \to (g_W/2\cos\theta_W)\gamma_\mu(c_V - c_A\gamma_5)$ as

$$\Psi_{\lambda\lambda'}^{Z(\xi)}(\alpha, \boldsymbol{k}_\perp) = -\frac{g_W}{2\cos\theta_W} \times \frac{\sqrt{\alpha(1-\alpha)}\,\bar{u}_\lambda(k) \not\varepsilon^{(\xi)} (c_V - c_A\gamma_5) v_{\lambda'}(q-k)}{\alpha(1-\alpha)\mathcal{Q}^2 + \boldsymbol{k}_\perp^2 + m_Q^2}. \quad (3)$$

Next we proceed to the light-cone WFs for the η_Q meson, corresponding to Fig. 2(b). Again, it is convenient to exploit the correspondence with J/ψ electroproduction. The light-cone WFs for the heavy vector mesons $V = J/\psi, \Upsilon$ have been discussed in many works, but are still controversial in the treatment of subleading effects like the Fermi motion corrections [4,5,15], corrections to ensure the pure S-wave $Q\bar{Q}$ state [16], corrections via the Melosh rotation [17], etc. Here we employ the light-cone WFs for the vector meson given by [see Fig. 2(b)]

$$\Psi_{\lambda\lambda'}^{V(\varpi)*}(\alpha, \boldsymbol{k}_\perp) = \frac{\bar{v}_{\lambda'}(\tilde{q}-k)}{\sqrt{1-\alpha}} \gamma^\mu e_\mu^{(\varpi)*} \mathcal{R} \frac{u_\lambda(k)}{\sqrt{\alpha}} \frac{\phi^*(\alpha, \boldsymbol{k}_\perp)}{M_V}, \quad (4)$$

where $\tilde{q} = q + \Delta$, M_V, and $e_\mu^{(\varpi)}$ ($\varpi = 0, \pm 1$) are the momentum, mass, and polarization vector of the vector meson with $\tilde{q}^2 = M_V^2$, $e^{(\varpi)} \cdot \tilde{q} = 0$, and $e^{(\varpi)*} \cdot e^{(\varpi')} = -\delta_{\varpi\varpi'}$. $\mathcal{R} \equiv (1 + \tilde{\not q}/M_V)/2$ denotes the projection operator, $\mathcal{R}^2 = \mathcal{R}$, to ensure the S-wave $Q\bar{Q}$ state in the heavy-quark limit [2,15,18]. (This projection operator coincides with that discussed in Ref. [16] up to the binding-energy effects of the quarkonia.) Note that Eq. (4) reduces to the vector meson WFs of Ref. [3] by the replacement $\mathcal{R} \to 1$. The physical interpretation of Eq. (4) is similar to the "perturbative" WFs (2) and (3), but the scalar function $\phi(\alpha, \boldsymbol{k}_\perp)$ contains nonperturbative dynamics between Q and $\bar{Q}$. Now, the light-cone WFs for the η_Q meson can be derived from Eq. (4) by utilizing spin symmetry, which is exact in the heavy-quark limit. This symmetry relates the four degenerate S-wave states, i.e., η_Q and the three spin states of the vector meson [19], namely, $M_{\eta_Q} = M_V$, and the pseudoscalar state is related to the vector state with longitudinal polarization as $|\eta_Q\rangle = 2\hat{S}_Q^3 |V(\varpi = 0)\rangle$, where $\hat{S}_Q^3$ is the third component of the Hermitian spin operator $\hat{S}_Q^i$ which acts on the spin of the heavy quark Q but does not act on $\bar{Q}$. For the WFs we get [see Eq. (4)]

$$\Psi_{\lambda\lambda'}^{\eta_Q *}(\alpha, \boldsymbol{k}_\perp) = \frac{\bar{v}_{\lambda'}(\tilde{q}-k)}{\sqrt{1-\alpha}} \gamma^\mu e_\mu^{(0)*} \mathcal{R}(2S^3) \frac{u_\lambda(k)}{\sqrt{\alpha}} \frac{\phi^*(\alpha, \boldsymbol{k}_\perp)}{M_V}$$
$$= -\frac{\bar{v}_{\lambda'}(\tilde{q}-k)}{\sqrt{1-\alpha}} \gamma_5 \mathcal{R} \frac{u_\lambda(k)}{\sqrt{\alpha}} \frac{\phi^*(\alpha, \boldsymbol{k}_\perp)}{M_{\eta_Q}}. \quad (5)$$

Here S^3 is the matrix representation of $\hat{S}^3_Q$ as $S^3 = \gamma_5 \tilde{q}\epsilon^{(0)}/(2M_V)$, which is related to the spin matrix $\sigma^{12}/2 = \gamma_5\gamma^0\gamma^3/2$ in the meson rest frame by a Lorentz boost in the third direction [19]. Thus the η_Q is described by the same nonperturbative WF $\phi(\alpha,\boldsymbol{k}_\perp)$ as the vector meson. Note that, due to the presence of $\mathcal{R}$, the "$Q\bar{Q}\eta_Q$ vertex" involves pseudovector as well as pseudoscalar coupling.

Combining our Z and η_Q WFs with the $Q\bar{Q}$-N elastic amplitude that was obtained in Ref. [3], we get the total amplitude for the polarization $\varepsilon^{(\xi)}$ of the Z boson as

$$\mathrm{Im}\mathcal{M}^{(\xi)} = \frac{\sqrt{2}\pi s}{2\sqrt{N_c}} \sum_{\lambda'\lambda} \int \frac{d\alpha d^2k_\perp}{16\pi^3} \int d^2 l_\perp \frac{\alpha_s(\boldsymbol{l}_\perp^2)}{\boldsymbol{l}_\perp^4} f(x,\boldsymbol{l}_\perp^2) \times[2\Psi^{Z(\xi)}_{\lambda\lambda'}(\alpha,\boldsymbol{k}_\perp) - \Psi^{Z(\xi)}_{\lambda\lambda'}(\alpha,\boldsymbol{k}_\perp+\boldsymbol{l}_\perp) - \Psi^{Z(\xi)}_{\lambda\lambda'}(\alpha,\boldsymbol{k}_\perp-\boldsymbol{l}_\perp)]\Psi^{\eta_Q}_{\lambda\lambda'}{}^{*}(\alpha,\boldsymbol{k}_\perp), \tag{6}$$

up to terms suppressed for high W and $\boldsymbol{\Delta}_\perp^2 \cong -t \to 0$. Here $\alpha_s(\boldsymbol{l}_\perp^2)$ denotes the running coupling constant for N_c colors. As usual, we have explicitly dealt with the imaginary part of the production amplitude, because the small real part can be reconstructed perturbatively [see Eq. (7) below]. $f(x,\boldsymbol{l}_\perp^2)$ denotes the unintegrated gluon density, and $x=(\mathcal{Q}^2+M^2_{\eta_Q})/s$ and $\boldsymbol{l}_\perp$ are the longitudinal momentum fraction and the transverse momentum, respectively, which are carried by a gluon inside the nucleon [3,5]. We substitute Eqs. (3) and (5) into Eq. (6) and go over to the "$\boldsymbol{b}$ space" conjugate to the $\boldsymbol{k}_\perp$ space via the Fourier transformation $\phi(\alpha,\boldsymbol{k}_\perp) = 4\pi\int d^2 b e^{-i\boldsymbol{k}_\perp\cdot\boldsymbol{b}}\phi(\alpha,\boldsymbol{b})$; $\boldsymbol{b}$ denotes the transverse separation between Q and $\bar{Q}$. Then, it is straightforward to see that $\mathrm{Im}\mathcal{M}^{(\pm1)}=0$, which reflects helicity conservation in the high energy limit. $\mathrm{Im}\mathcal{M}^{(0)}$ can be calculated in parallel with previous work for vector meson production [4,5,20]. In the integrand, there appear the terms $e^{i\boldsymbol{l}_\perp\cdot\boldsymbol{b}}$ and $e^{-i\boldsymbol{l}_\perp\cdot\boldsymbol{b}}$. The leading $\ln(\mathcal{Q}^2/\Lambda^2_{\mathrm{QCD}})$ contribution comes from the region $\Lambda^2_{\mathrm{QCD}} \ll \boldsymbol{l}_\perp^2 \ll \mathcal{Q}^2_{\mathrm{eff}}$ $(\equiv[\mathcal{Q}^2+M^2_{\eta_Q}]/4)$ of the $\boldsymbol{l}_\perp$ integral [3,5], where $\boldsymbol{l}_\perp\cdot\boldsymbol{b}\ll 1$ is satisfied because $|\boldsymbol{b}|\sim 1/m_Q$. We retain only the leading nonzero term in the power series in $\boldsymbol{l}_\perp\cdot\boldsymbol{b}$, which corresponds to the "color-dipole picture" [4,20]. Then, using $\int^{\mathcal{Q}^2_{\mathrm{eff}}} dl^2_\perp f(x,\boldsymbol{l}_\perp^2)/\boldsymbol{l}_\perp^2 = xG(x,\mathcal{Q}^2_{\mathrm{eff}})$ with $G(x,\mathcal{Q}^2_{\mathrm{eff}})$ the conventional gluon distribution, we get $(b\equiv|\boldsymbol{b}|)$ [20]

$$i\mathcal{M}^{(0)} = \frac{-\sqrt{2}\pi^2 W^2}{\sqrt{N_c}} \frac{g_W m_Q c_A}{M_{\eta_Q}\mathcal{Q}\cos\theta_W} \alpha_s(\mathcal{Q}^2_{\mathrm{eff}})\left[1+i\frac{\pi}{2}\frac{\partial}{\partial \ln x}\right] \times xG(x,\mathcal{Q}^2_{\mathrm{eff}})\int_0^1 \frac{d\alpha\mathcal{Q}_m}{\alpha(1-\alpha)} \times\int_0^\infty dbb^2\phi^*(\alpha,b)K_1(b\mathcal{Q}_m), \tag{7}$$

where $\mathcal{Q}_m = [\alpha(1-\alpha)\mathcal{Q}^2+m_Q^2]^{1/2}$, K_1 is a modified Bessel function, and we have included the real part of the amplitude as a perturbation [3–5]. As expected, the result (7) is proportional to c_A, so that the η_Q meson is generated by the axial-vector part of the weak current.

For comparison, we also calculate the diffractive vector meson production via the weak neutral current, by the replacement $\Psi^{\eta_Q}_{\lambda\lambda'} \to \Psi^{V(\varpi)}_{\lambda\lambda'}$ in Eq. (6). Substituting Eq. (4), we find that $\xi=\varpi$, i.e., $\mathcal{M}^{(0)}$ and $\mathcal{M}^{(\pm1)}$ give the production of the longitudinally and transversely polarized vector mesons, respectively, and that all these amplitudes are proportional to the vector coupling c_V. [When we replace the factor $g_W c_V/(2\cos\theta_W)$ by $e_c=2e/3$ in these results, we obtain amplitudes $\mathcal{M}^{(\xi)}$ identical to those for the diffractive electroproduction of J/ψ [4,5], up to the corrections due to $\mathcal{R}$ of Eq. (4).]

Combining Eq. (7) with the Z boson propagator and the weak neutral current by a neutrino, the forward differential cross section for the η_Q production is given by

$$\left.\frac{d^3\sigma(\nu N\to\nu' N'\eta_Q)}{dsd\mathcal{Q}^2dt}\right|_{t=0} = \frac{1}{4(8\pi)^3E_\nu^2M_N^2 s}\frac{g_W^2}{\cos^2\theta_W} \times\frac{\mathcal{Q}^2}{(\mathcal{Q}^2+M_Z^2)^2}\frac{\epsilon}{1-\epsilon}|\mathcal{M}^{(0)}|^2, \tag{8}$$

where E_ν is the neutrino beam energy in the laboratory system, and $\epsilon=[4(1-y)-Q^2/E_\nu^2]/[2\{1+(1-y)^2\}+Q^2/E_\nu^2]$ with $y=s/(2M_N E_\nu)$ is the polarization parameter of the virtual Z boson [7,12]. In order to evaluate the corresponding elastic η_Q production rate, we assume the t dependence as $d^3\sigma/dsd\mathcal{Q}^2dt = d^3\sigma/dsd\mathcal{Q}^2dt|_{t=0}\exp(B_{\eta_Q}t)$ with a constant diffractive slope, as in the case of vector meson production. Integrating $d^2\sigma/dsd\mathcal{Q}^2 = (1/B_{\eta_Q})d^3\sigma/dsd\mathcal{Q}^2dt|_{t=0}$ over $\mathcal{Q}^2$ and s, we get the elastic production rate $\sigma(\nu N\to\nu' N'\eta_Q)$ as a function of E_ν.

For numerical computation of $\sigma(\nu N\to\nu' N'\eta_Q)$, we need the explicit form of $\phi(\alpha,\boldsymbol{b})$ of Eq. (7). From Eqs. (4) and (5), we can use the corresponding nonperturbative part of the vector meson WF which was constructed in previous work based on, e.g., the nonrelativistic potential model for heavy quarkonia [4,20]. In this work, we adopt the WF from the Cornell potential model with the corresponding quark masses $m_c=1.5$ GeV, $m_b=4.9$ GeV [21]. A procedure to construct $\phi(\alpha,\boldsymbol{k}_\perp)$ with the light-cone variables from the usual Schrödinger WF $\phi_{NR}(\boldsymbol{k})$ has been given in Refs. [4,20]. Also, we use the empirical values for the masses $M_{\eta_c}=2.98$ GeV, $M_N=0.94$ GeV, and $M_Z=91.2$ GeV. For η_b, we use $M_{\eta_b}=9.45$ GeV estimated in Ref. [22]. Because the slope B_{η_Q} introduced above is unknown, we assume that B_{η_Q} has the same value as that for the corresponding vector meson: $B_{\eta_c}=4.5\ \mathrm{GeV}^{-2}$ from the experimental value for J/ψ [5] and $B_{\eta_b}=3.9\ \mathrm{GeV}^{-2}$ following the value for Υ in Ref. [23]. For the gluon distribution $G(x,\mathcal{Q}^2_{\mathrm{eff}})$ of Eq. (7), we employ the GRV95 next-to-leading order parametrization [24].

We show the elastic η_c production rate, $\sigma(\nu N\to\nu' N'\eta_c)$, by the solid curve in Fig. 3. The result monotonically increases as a function of the beam energy E_ν. Such behavior is similar with that observed in the

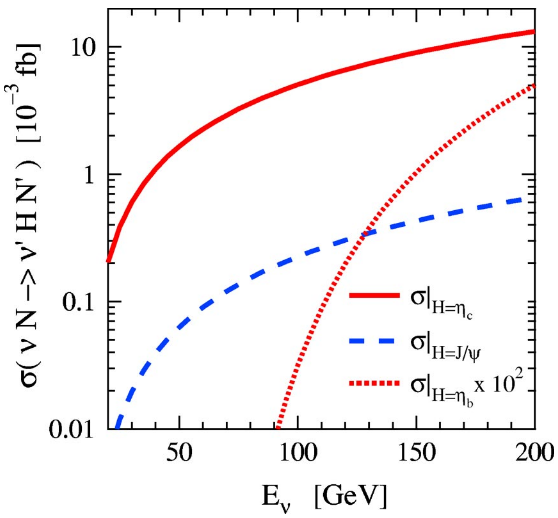

FIG. 3. (Color online) The elastic production rates as functions of E_ν. Solid, dashed, and dotted curves are for η_c, J/ψ, and η_b, respectively. Note that the dotted curve shows the rate multiplied by 10^2.

π-production data by neutral [7] and charged currents [9]. For comparison, we show the elastic J/ψ production rate $\sigma(\nu N \rightarrow \nu' N' J/\psi)$ by the dashed curve [see the discussion below Eq. (7)] [25]. The rate for η_c production is much larger than that for J/ψ by a factor ~ 20. This is mainly due to the relevant weak couplings, c_A for η_c and c_V for J/ψ, as $(c_A/c_V)^2 \cong 7$. Another important effect comes from the different behavior of the Z light-cone WFs (3) between the axial-vector and vector channels: It is straightforward to see that the η_c diffractive amplitude (7) as well as the corresponding amplitudes for the longitudinally and transversely polarized J/ψ decrease rather rapidly for the high $\mathcal{Q}^2$ region, $\mathcal{Q}^2 \gtrsim 4m_c^2$, so that the elastic production rates are in principle dominated by the low $\mathcal{Q}^2$ contribution of the differential cross sections (similar behavior is observed also for J/ψ electroproduction [4,5]). For weak neutral current processes, however, a typical factor $\mathcal{Q}^2/(\mathcal{Q}^2+M_Z^2)^2$ appears in the differential cross sections as in Eq. (8). The low $\mathcal{Q}^2$ contribution of the differential cross section for J/ψ is suppressed by this factor, while that for η_c avoids the suppression due to the $\sim 1/\mathcal{Q}$ behavior of Eq. (7). This particular behavior of the η_c diffractive amplitude comes from the spinor matrix element of the Z light-cone WFs (3) as $\overline{u_\lambda}(k)\not{\epsilon}^{(0)}\gamma_5 v_{\lambda'}(q-k) \sim 1/\mathcal{Q}$ for $\mathcal{Q}\rightarrow 0$. On the other hand, $\overline{u_\lambda}(k)\not{\epsilon}^{(0)} v_{\lambda'}(q-k) \sim \mathcal{Q}$ and $\overline{u_\lambda}(k)\not{\epsilon}^{(\pm 1)} v_{\lambda'}(q-k) \sim$ const, for the vector channels relevant for J/ψ.

In Fig. 3, we also show the η_b production rate $\sigma(\nu N \rightarrow \nu' N' \eta_b)$ by the dotted curve. Although the rate for η_b is generally much smaller than that for η_c, the former increases more rapidly than the latter for increasing E_ν. Therefore, the η_b production rate could become comparable with the η_c production for higher beam energy, suggesting the possibility of observing η_b through the diffractive production by high intensity neutrino beams available in ongoing or forthcoming neutrino facilities.

In conclusion, we have computed the diffractive production cross sections of $\eta_{c,b}$ mesons via the weak neutral current, using the new results for the light-cone WFs for Z and $\eta_{c,b}$. Our results demonstrate that neutrino-induced production will open a new window to measure $\eta_{c,b}$.

We are pleased to acknowledge useful discussions with T. Hatsuda and H. Mineo at the early stage of this work. One of the authors (A.H.) is grateful to T. Hirano for his support with the numerical calculation. A.H. is supported by the JSPS.

[1] H. Abramowicz, Int. J. Mod. Phys. A **15S1**, 495 (2000).
[2] M.G. Ryskin, Z. Phys. C **57**, 89 (1993).
[3] S.J. Brodsky, L. Frankfurt, J.F. Gunion, A.H. Mueller, and M. Strikman, Phys. Rev. D **50**, 3134 (1994).
[4] L. Frankfurt, W. Koepf, and M. Strikman, Phys. Rev. D **57**, 512 (1998).
[5] M.G. Ryskin, R.G. Roberts, A.D. Martin, and E.M. Levin, Z. Phys. C **76**, 231 (1997).
[6] E.M. Levin, A.D. Martin, M.G. Ryskin, and T. Teubner, Z. Phys. C **74**, 671 (1997).
[7] B.Z. Kopeliovich and P. Marage, Int. J. Mod. Phys. A **8**, 1513 (1993).
[8] J. Pumplin and W. Repko, Phys. Rev. D **12**, 1376 (1975).
[9] E815 Collaboration, T. Adams *et al.*, Phys. Rev. D **61**, 092001 (2000).
[10] E632 Collaboration, S. Willocq *et al.*, Phys. Rev. D **47**, 2661 (1993).
[11] CHORUS Collaboration, P. Annis *et al.*, Phys. Lett. B **435**, 458 (1998).
[12] J.H. Kühn and R. Rückl, Phys. Lett. **95B**, 431 (1980).
[13] B. Lehmann-Dronke and A. Schäfer, Phys. Lett. B **521**, 55 (2001).
[14] S. Gieseke and C.-F. Qiao, Phys. Rev. D **61**, 074028 (2000).
[15] P. Hoodbhoy, Phys. Rev. D **56**, 388 (1997).
[16] I.P. Ivanov and N.N. Nikolaev, JETP Lett. **69**, 294 (1999).
[17] J. Hüfner, Yu.P. Ivanov, B.Z. Kopeliovich, and A.V. Tarasov, Phys. Rev. D **62**, 094022 (2000).
[18] E.L. Berger and D.L. Jones, Phys. Rev. D **23**, 1521 (1981).
[19] H. Georgi, Phys. Lett. B **240**, 447 (1990); T. Mannel and G.A. Schuler, *ibid.* **349**, 181 (1995).
[20] K. Suzuki, A. Hayashigaki, K. Itakura, J. Alam, and T. Hatsuda, Phys. Rev. D **62**, 031501(R) (2000).
[21] E.J. Eichten and C. Quigg, Phys. Rev. D **52**, 1726 (1995).
[22] D.S. Hwang and G.-H. Kim, Z. Phys. C **76**, 107 (1997).
[23] L. Frankfurt, M. McDermott, and M. Strikman, J. High Energy Phys. **02**, 002 (1999).
[24] M. Glück, E. Reya, and A. Vogt, Z. Phys. C **67**, 433 (1995).
[25] The vector dominance model [11] gives $\sigma(\nu N \rightarrow \nu' N' J/\psi) \simeq 10^{-2}$ fb for $E_\nu = 100$ GeV with similar E_ν dependence as our QCD result (dashed curve). At present, we do not have enough experimental data [8] to be compared with these theoretical predictions.